International Journal of Pressure Vessels and Piping 149 (2017) 108–119

Contents lists available at ScienceDirect

International Journal of Pressure Vessels and Piping

journal homepage: www.elsevier.com/locate/ijpvp

Experimental and numerical study of steel pipe with part-wall defect reinforced with fibre glass sleeve

Lukasz Mazurkiewicz [a], Michal Tomaszewski [a], Jerzy Malachowski [a, *], Kamil Sybilski [a], Mikhail Chebakov [b], Maciej Witek [c], Peter Yukhymets [d], Roman Dmitrienko [d]

[a] Department of Mechanics and Applied Computer Science, Faculty of Mechanical Engineering, Military University of Technology, 2 Gen. Kaliskiego Street, 00-908 Warsaw, Poland
[b] Institute of Mathematics, Mechanics and Computer Science, Southern Federal University, 200/1 Stachki Avenue, Rostov-on-Don 344090, Russia
[c] Department of Thermal and Gas Engineering Systems, Faculty of Building Services, Hydro- and Environmental Engineering, Warsaw University of Technology, 20 Nowowiejska St., 00-653 Warsaw, Poland
[d] The E. O. Paton Electric Welding Institute, 11 Bozhenko Str., Kiev 03680, Ukraine

ARTICLE INFO

Article history:
Received 17 March 2016
Accepted 20 December 2016
Available online 24 December 2016

Keywords:
Burst pressure tests
Seamless hot-rolled steel pipe
Corrosion defect
Glass fibre composite repair
FE analysis
Experimental tests

ABSTRACT

The paper presents numerical and experimental burst pressure evaluation of the gas seamless hot-rolled steel pipe. The main goal was to estimate mechanical toughness of pipe wrapped with composite sleeve and verify selected sleeve thickness. The authors used a nonlinear explicit FE code with constitutive models which allows for steel and composite structure failure modelling. Thanks to the achieved numerical and analytical results it was possible to perform the comparison with data received from a capacity test and good correlation between the results were obtained. Additionally, the conducted analyses revealed that local reduction of pipe wall thickness from 6 mm to 2.4 mm due to corrosion defect can reduce high pressure resistance by about 40%. Finally, pipe repaired by a fibre glass sleeve with epoxy resin with 6 mm thickness turned out more resistant than an original steel pipe considering burst pressure.

1. Introduction

The main goal of the gas grid maintenance is to avoid leaks and raptures that may result in a fire of flammable clouds and lead to environmental consequences in the surrounding area. High pressure gas pipeline failure may cause also injuries and human fatalities. To reduce failure probability while at the same time keeping gas transmission system design capacity, the pipeline technical condition is periodically controlled by in-line inspections collecting and sizing defects [1,2]. Consequently other scheduled maintenance activities such as: pipeline route surveillance, checks of tightness of the pipeline, corrosion prevention and pressure monitoring, are applied by the operator. Part-wall metal loss defect of buried pipelines are mostly a consequence of electrochemical corrosion caused by oxidation, either direct or alternating current at locations of damaged insulation, sometimes are caused by third party interference. External and internal steel pipe wall thickness losses without any reinforcement were calculated analytically taking into consideration pipeline safe operating pressure in many publications starting from early 1970s [1,3,4]. Many researchers studied stress and strain in pressurised cylindrical shells with and without defects in various loading condition using numerical algorithms based on a finite element method [5–9].

Repairs of the existing damage or complete replacement of the pipe segment are performed in case of defects exceed code-based thresholds [10]. During oil/gas pipeline operation and maintenance activities, replacements of the pipe segments are complicated as it requires a pause in the fluid transport and distribution, which can generate substantial expenditures or income losses. For the above mentioned reason, the most important issue for the operator of oil/gas pipeline is to apply a complex approach to inspection-repair policy and to find cost effective repair technologies to maintain pipeline reliability. Pipelines with part-wall metal loss defects can be reinforced with a sleeve by wrapping it with

* Corresponding author.
E-mail addresses: lukasz.mazurkiewicz@wat.edu.pl (L. Mazurkiewicz), michal.tomaszewski@wat.edu.pl (M. Tomaszewski), jerzy.malachowski@wat.edu.pl (J. Malachowski), kamil.sybilski@wat.edu.pl (K. Sybilski), chebakov@math.sfedu.ru (M. Chebakov), maciej_witek@is.pw.edu.pl (M. Witek), yupeter@ukr.net (P. Yukhymets), dri1@ukr.net (R. Dmitrienko).

http://dx.doi.org/10.1016/j.ijpvp.2016.12.008
0308-0161/

concentric cylinders of composite material and application of a cohesive epoxy filler. Different kinds of applied commercial fibre based reinforcements are shown in publication [11]. The basic idea of the reinforcement techniques is to transfer hoop stress from the defected area of the steel pipe caused by the internal fluid pressure to the composite sleeve. An internally corroded pipeline may be also locally reinforced by the sleeve covering defect spots area. Nevertheless, composite repair systems are not effective for through-thickness corrosion defects since due to a fluid spill. The most important variable to define an adequate sleeve is to select required thickness and a number of layers for different composite systems. There are only few publications in the area of mechanical analysis of steel pipelines with hoop reinforced pipe wall with composite repair systems [12–14]. A recently published paper [15] provides an analytical methodology based on widely known criteria (i.a. ASME B31G criterion, RSTRENG 0.85, DNV-RP-F-101) to estimate the failure pressure when a pipe is repaired with polymer based composite cylinder.

The present paper aims at numerical calculations of a thin-wall steel pipe defected by corrosion and reinforced with a fibre glass composite sleeve. The main goal of this study is to compare numerical calculation results of pipe burst pressure with data received from a destructive strength test. It was assumed in the research that, from the point of view of mechanical strength, the repaired pipeline could be equally or more resistant to pressure compared to a pipe without any defects. The results of the paper are calculations of mechanical toughness of a steel pipe wrapped with a cylindrical composite sleeve and verification of selected sleeve thickness (number of fibre glass layers) are the key parameters for burst pressure solutions.

2. Object of study

The object of present research was a high pressure gas seamless hot-rolled pipe made of grade 20 steel according to technical requirements of the Standard GOST 8731-74 [16]. The pipe outside diameter was 219 mm and wall thickness 6 mm. For this research the pipeline segment with length of a 1 m, damaged by external part-wall metal loss defect, was considered.

To repair the pipeline, a composite sleeve made of fibre glass and epoxy filler was proposed. The length of the repair was approx. 50 mm longer than the surface defect. A composite sleeve with unidirectional layers was considered. Glass reinforcement was carried out in the circumferential direction. In order to investigate the effectiveness of composite repair considering burst pressure, several configurations of pipelines were taken into consideration:

- pipeline without defect (Case 1),
- pipeline with defect without repair (Case 2),
- pipeline without defect and with repair sleeve (Case 3),
- pipeline with defect and repair sleeve (Case 4).

3. Materials and methods

3.1. Experimental steel tests

The pipeline steel corresponds to steel PSL 2 Level which is commonly used in petroleum and natural gas transportation according to the Standard PN-EN-ISO 3183 [17]. Chemical composition of the modern steel for oil and gas industry, the manufacturing process, and also properties of steel designed for pipes to be used for construction of transmission pipelines are presented in the publication [18]. The manufacturing process of the pipe consists in rolling steel sheets to achieve a desirable shape [19]. The rolling process allows obtaining a certain material structure. Such a structure effects the crystal seeds size, which influences various parameters depending on the direction of inducted stress (anisotropy of the material). A broader description of the problem can be found in Ref. [20].

Authors conducted several experimental tests to investigate the material properties of the steel. Experimental tests consisted in uniaxial tensile tests of samples cut out from the pipe in both axial and circumferential directions. The difference between strength properties from both tests was less than 5%, therefore in further discussion the material was assumed as isotropic. The strength properties form tests of stretching in circumferential direction as a dominating stress state for internal pressure loading were used. For the needs of numerical analyses, the obtained stress-strain data were transformed from standard engineering to real values using the following formulas which are valid until necking [21,22]:

$$\varepsilon = \ln(1 + \varepsilon_{eng}) \tag{1}$$

$$\sigma = \sigma_{eng}(1 + \varepsilon_{eng}) \tag{2}$$

where: σ_{eng}, ε_{eng} – engineering stress and strain from uniaxial tests; σ, ε – real stress and strain (see Fig. 1).

The obtained material parameters used in the current analysis are shown in Table 1 and the plasticity range was defined through the use of the plasticity range curve (Fig. 2).

3.2. Experimental pipe testing

During the experiments, a pipe with diameter 219 mm and wall thickness 6 mm made of 20 steel type was subjected to pressure stress with the use of water injected into the pipe with a hydraulic pump (Fig. 3) [23]. Loading the specimen by internal pressure was carried out in steps. In the end of analysis the pressure was released to 0.

Four burst pressure loading experimental tests corresponding to case 1÷4 were performed. The first test (Fig. 4a) was performed on a pipe without defect. During the second experiment (Fig. 4b), a pipe was modified and had a surface defect imitating corrosion defect of the pipe. In the next experiment, a pipe without defect was wrapped in a composite sleeve (Fig. 4c). After wrapping, in order to measure composite thickness, a strip of composite was cut out at around 1/3 of the pipe length. The measured composite sleeve thickness was 2.5 mm. The last experiment (Fig. 4d) considered a pipe with defect (corresponding to the pipe from the second test), filler with epoxy resin and was wrapped with a glass fibre reinforced composite sleeve.

The results of experimental tests used in this study were the maximum pressures that the specimens sustained.

Table 1
Material properties for Steel 20 [20].

Density [kg/mm^3]	Young modulus [GPa]	Poisson ratio [-]	Yield strength [MPa]	Failure strain [-]
7.830e-9	200	0.3	305	0.33

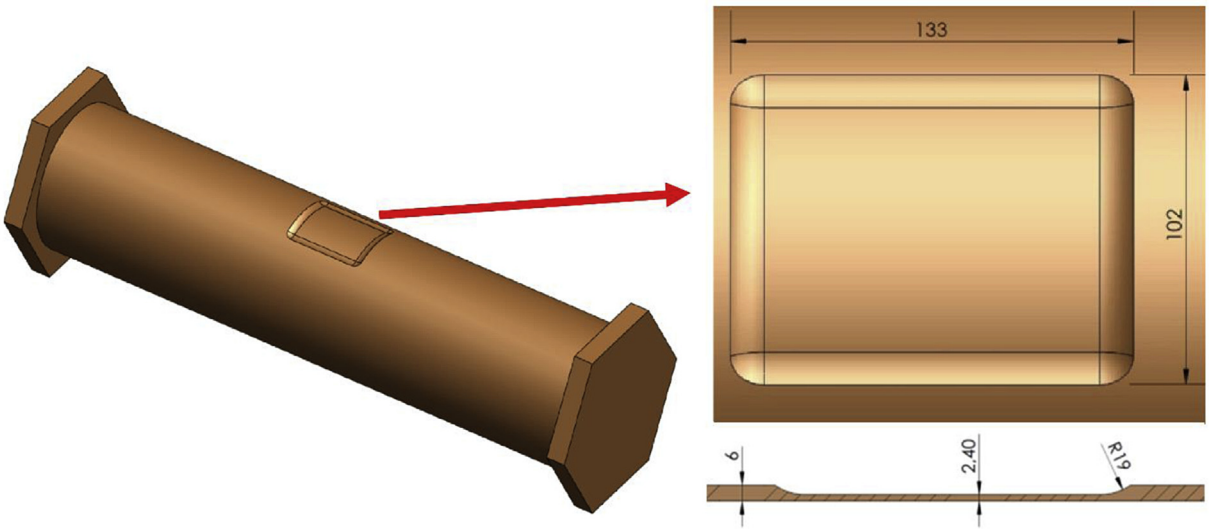

Fig. 1. Geometry of pipe damaged by external part-wall metal loss defect.

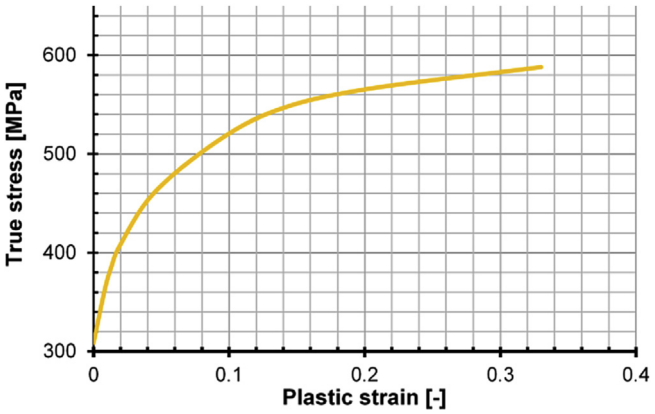

Fig. 2. True stress vs plastic strain of Steel 20.

3.3. Numerical analyses

Numerical studies of pipeline burst pressure testing due to highly nonlinear behaviour during the fracture process were carried out using FE software with an explicit integration procedure. The explicit dynamics procedure uses explicit central difference time integration and the equation solved has the following form [24]:

$$M\ddot{x}_n = F_n^{ext} - F_n^{int} - C\dot{x}_n \tag{3}$$

where: M – diagonal mass matrix; F_n^{ext} – vector of external forces; F_n^{int} – vector of internal forces, C – dumping matrix; , $\dot{x}_n$, $\ddot{x}_n$ – velocity and acceleration vectors.

3.3.1. Steel constitutive model

The piecewise linear plasticity material model based on the test data acquired from tensile tests was used for steel description. In this model a yield function is given by Ref. [24]:

$$\phi = \frac{1}{2}s_{ij}s_{ij} - \frac{\sigma_y^2}{3} \le 0 \tag{4}$$

where: ϕ – yield function; s – deviatoric Cauchy stress; σ_y – yield stress.

3.3.2. Airbag model for pressure loading

In the numerical model, to consider pressure changes with deformations of the pipe during inflation, the simple airbag algorithm was used, in which pressure is defined by equation [24]:

$$p = \left(\frac{c_p}{c_v} - 1\right)\rho\, e \tag{5}$$

where: c_p – heat capacity at constant pressure; c_v – heat capacity at constant volume; ρ – density; e – specific internal energy of the gas (Table 2).

The filling of the airbag was realized by a specifying input mass flow rate.

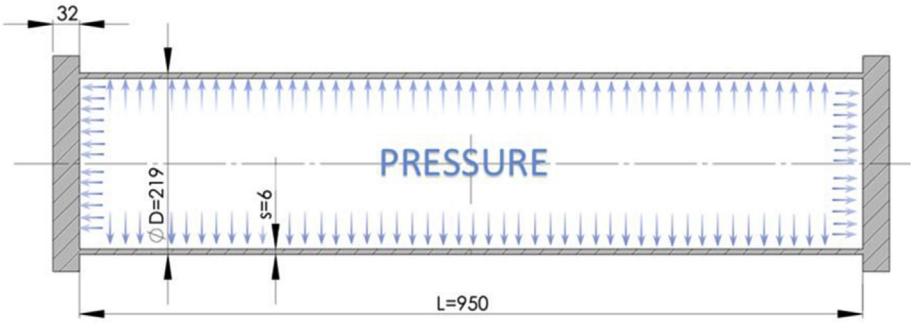

Fig. 3. Experimental test set-up.

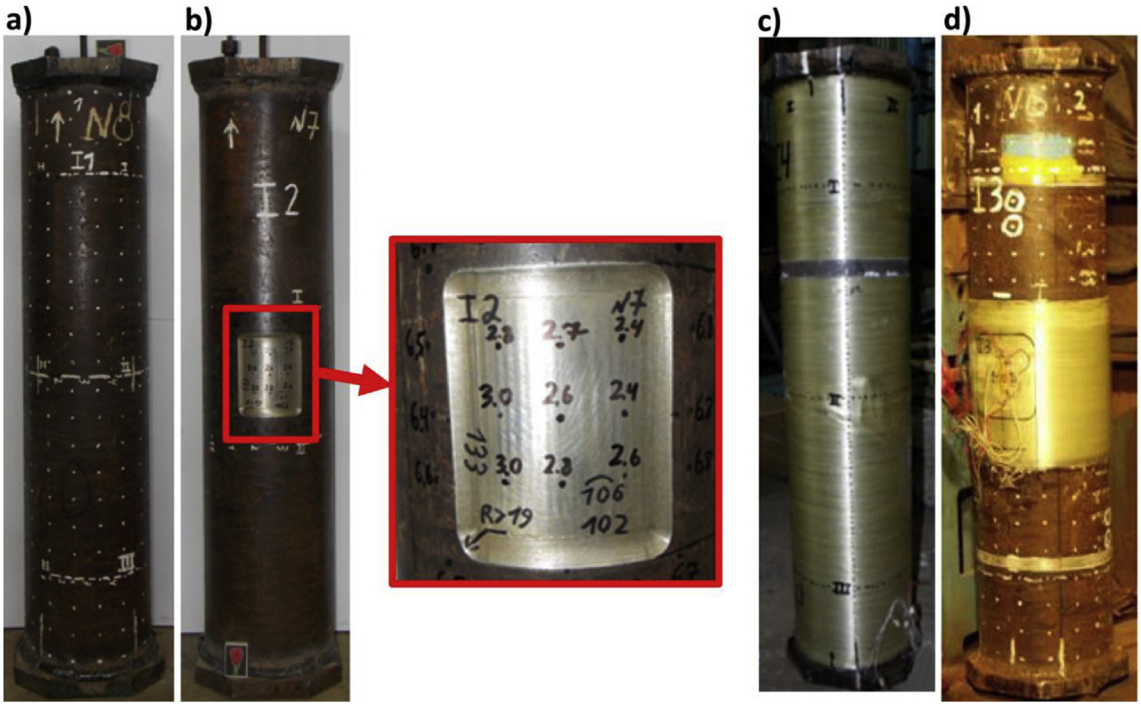

Fig. 4. Experimental test samples for each case: a) case 1, b) case 2, c) case 3, d) case 4.[23]

3.3.3. Composite material model

From the number of composite materials models available in the LS-Dyna code, the material model specially designated to model failure mechanisms observed in composite materials was chosen to describe the layers of the composite sleeve. The model was based on the following failure modes criteria [25,26]:

For the tensile fibre mode.

$$\sigma_{aa} > 0 \quad then \quad e_f^2 = \left(\frac{\sigma_{aa}}{X_t}\right)^2 + \left(\frac{\sigma_{ab}}{S_c}\right)^2 - 1 \begin{cases} \geq 0 \; failed \\ < 0 \; elastic \end{cases} \qquad (6)$$

$$E_a = E_b = G_{ab} = \nu_{ba} = \nu_{ab} = 0$$

For the compressive fibre mode.

$$\sigma_{aa} < 0 \quad then \quad e_c^2 = \left(\frac{\sigma_{aa}}{X_c}\right)^2 - 1 \begin{cases} \geq 0 \; failed \\ < 0 \; elastic \end{cases} \qquad (7)$$

$$E_a = \nu_{ba} = \nu_{ab} = 0$$

For the tensile matrix mode.

$$\sigma_{bb} > 0 \; then \; e_m^2 = \left(\frac{\sigma_{bb}}{Y_t}\right)^2 + \left(\frac{\sigma_{ab}}{S_c}\right)^2 - 1 \begin{cases} \geq 0 \; failed \\ < 0 \; elastic \end{cases} \qquad (8)$$

$$E_b = G_{ab} = \nu_{ba} = 0$$

For the compressive matrix mode.

Table 2
Properties for airbag model [24].

c_v [J/cm^{3}K]	c_p [J/gK]	ρ [kg/m^3]
4.18	4.181	1000

$$\sigma_{bb} < 0 \; then \; e_d^2 = \left(\frac{\sigma_{bb}}{2S_c}\right)^2 + \left[\left(\frac{Y_c}{2S_c}\right)^2 - 1\right]\frac{\sigma_{bb}}{Y_c} - 1 \begin{cases} \geq 0 \; failed \\ < 0 \; elastic \end{cases}$$

$$E_b = G_{ab} = \nu_{ba} = \nu_{ab} = 0 \qquad (9)$$

where: e_f, e_c, e_m and e_d failure indexes; σ_{aa} and σ_{bb} – stress in longitudinal and transverse direction; σ_{ab} – in plane shear stress; X_t and Y_t – longitudinal and transverse tensile strength; X_c and Y_c – longitudinal and transverse compressive strength; S_c – shear strength; E_a and E_b – Young modulus in longitudinal and transverse direction; G_{ab} – shear modulus;

In the material model, erosion can also occur when the tensile fibre strain is greater than ε^{+}_{max} or smaller than ε^{-}_{max} and when the effective strain is greater than ε_{fs}. When failure occurs in all of the composite layers (through-thickness integration points), the element is deleted. The material constants are taken from literature and identification tests [23] (Table 3).

3.3.4. Filler

The filler of the defect volume was made of epoxy resin. The behaviour of filler was described by an elasto-plastic material model with an arbitrary stress versus strain curve (Fig. 5) [24]. Additionally, a volumetric strain failure criterion in compression was applied (Table 4.where: ρ – density; E – Young modulus; ν – Poisson ratio; ε^{+}_{fail} – failure strain in tension; ε^{-}_{vol} –volumetric failure strain in compression if volumetric strain is calculated as $\varepsilon_{vol} = \varepsilon_1 + \varepsilon_2 + \varepsilon_3$.

The interlaminar connection in the composite and between the composite and the filler/pipe was described using cohesive interface with a bilinear traction-separation law and a quadratic mixed mode delamination criterion.

3.3.5. Discrete model

For each analysis case, the discrete models were developed. In

Table 3
Material properties for fibre glass reinforced composite [23].

ρ [kg/m^3]	E_a [GPa]	$E_b = E_c$ [GPa]	$\nu_{ba} = \nu_{ca}$ [-]	ν_{cb} [-]	$G_{ab} = G_{ca}$ [MPa]	G_{cb} [MPa]	ε_{fs} [-]
1800	48.47	6.77	0.099	0.40	3.2	1.67	0.2
X_c [MPa]	X_t [MPa]	Y_c [MPa]	Y_t [MPa]	S_c [MPa]	$Y_{c\,fail}$ [-]	$\varepsilon_{max}+$ [-]	$\varepsilon_{max}-$ [-]
320	678.5	110	34.4	45.8	2	0.1	−0.1

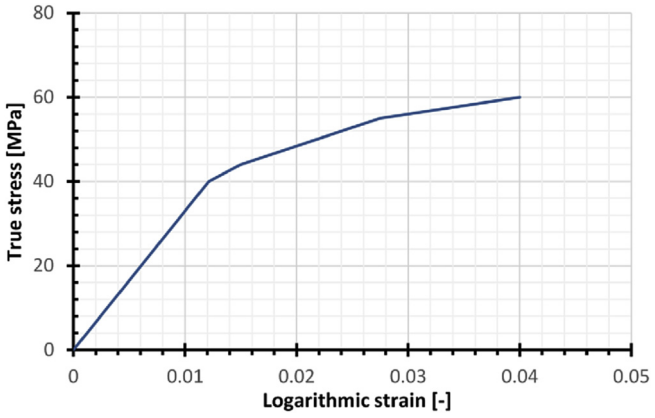

Fig. 5. True stress-strain curve for filler material model.

Table 4
Material properties for epoxy filler [26].

ρ [kg/m^3]	E [GPa]	ν [-]	ε^{+}_{fail} [-]	ε^{-}_{vol} [-]
1200	3.3	0.37	0.04	−0.7

order to simplify and to reduce the computational time, a symmetry of the problem was assumed and 1/8 of the model in all cases was taken into consideration. An FE model of the pipeline was developed using thick shell 8-noded elements with 5 through thickness integration points based on a full 3D constitutive law [27] and full integrated 8-noded brick elements for pipe lid. The size and type of pipe elements were based on investigations performed on a simplified model without defect. The loading was realized by an airbag expanding inside the pipe, which allows considering pressure changes with deformations of the pipe during inflation. The model statistics are presented in Table 5.(see Fig. 6)

4. Constitutive material model correlation

In order to validate a defined constitutive model, a numerical tension test of a steel sample [28] was performed. Geometry and dimensions of the sample are presented in Fig. 7.

The engineering stress-strain relation calculated from numerical simulation and the experimental test were compared (Fig. 8). It can be observed that good agreement between these curves was obtained. Authors assumed that the constitutive material model used to described steel 20 material is validated.

Table 5
Number of elements of developed FE models.

	Case 1	Case 2	Case 3	Case 4
Steel pipe – Tshell elements	99 264	92 088	99 264	81 936
Steel pipe lid – Solid elements	90 000	41 568	90 000	5196
Composite and filler – Solid elements	-	-	23 688	17 884

5. Results of experimental and numerical evaluation of burst pressure

The overall response of the pipe with and without composite wrap was obtained from the carried out analyses. In the following subsection, the results for each case are presented.

5.1. Pipe without defect

As a result of the experimental tests, the first pipe without defect sustained burst pressure (maximum pressure until failure) is equal to 27.59 MPa. The value of pressure for such a pipe type can be also calculated from the analytical formula shown below [22].

$$P_I = \frac{2}{\sqrt{3}} \frac{As_0}{r_0 \exp(m)} \left(\frac{m}{\sqrt{3}}\right)^m = 28.413MPa \tag{10}$$

where: s_O – pipe wall thickness; r_O – pipe outside radius; A, m – coefficients from σ-ε plastic range approximation by equation $\sigma = A\varepsilon^m$, where $A = \frac{\sigma_{02}}{\varepsilon_{02}{}^m}$.

The results of numerical analysis – pressure vs maximum radial displacement and the circumferential stress before and after failure are presented in Figs. 9 and 10.

The maximum burst pressure obtained from numerical calculations is 28.2 MPa and pressure at yield is 19.9 MPa. It can be observed that in booth numerical and experimental studies the similar fracture parallel to the axis of the pipe occurred. Due to the discrete model symmetry, constant thickness and perfectly isotropic material behaviour, more than one fracture starts to propagate. The small differences between the numerical/analytical and experimental results (Table 6) may result from the simplification used and initial boundary conditions. The pipe used in the experiment had non-uniform thickness ranging from 5.9 mm to 7.3 mm, which results from an imperfect manufacturing process, whereas in numerical and analytical calculations nominal thickness of 6 mm was assumed.

5.2. Pipe with part-wall defect without reinforcement

The second analysis considered the pipe with surface defect. The locally reduced thickness results in significant burst pressure reduction. The maximum pressure until failure obtained from numerical analysis dropped from 28.2 MPa for undamaged pipe to 17 MPa (Fig. 11). The value of pressure at failure for experimental trial is equal to 13.8 MPa [23]. The difference between results (Table 7) may be influenced by many variables – quality of material, especially after a machining process or non-uniform thickness in the segment where defect is located. The pressure value at which the strain approaches yield limit is 7.9 MPa. The value of pressure for such a pipe type can be also calculated from the analytical formula shown below [29]:

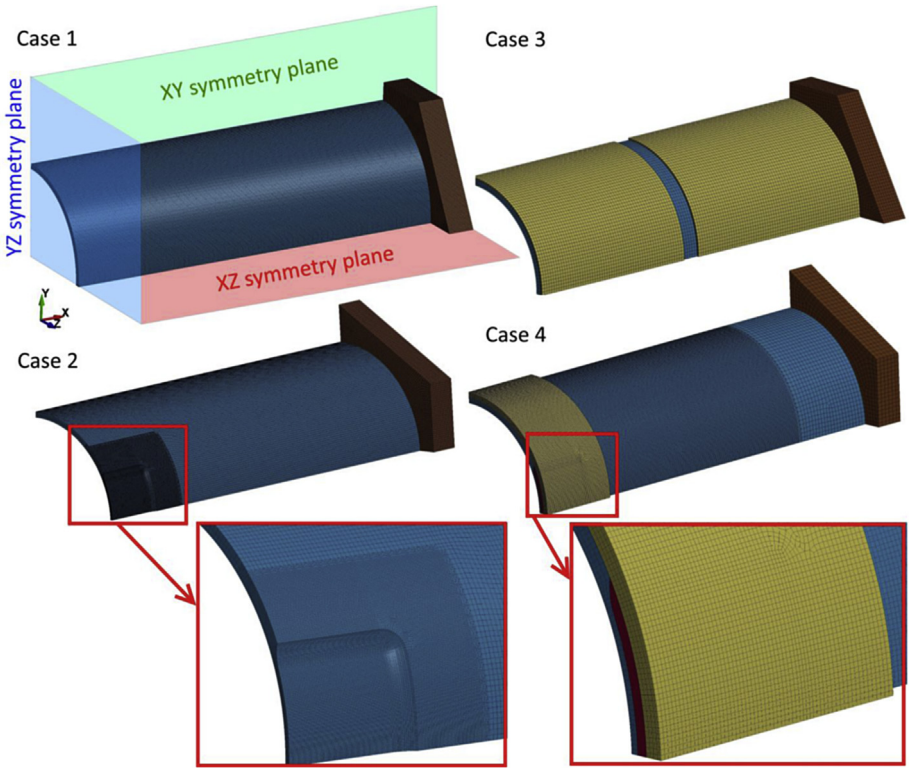

Fig. 6. FE models of pipe for analysed cases.

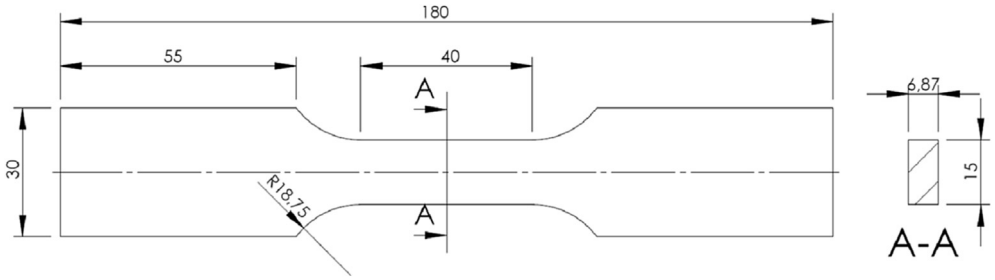

Fig. 7. Scheme of steel sample used in identification tensile tests.[28]

$$P_{II} = 1.05\frac{2\,s_0\sigma_u}{2r_0 - s_0}\frac{1-\frac{d}{s_0}}{1-\frac{d}{Qs_0}} = 15.26\,MPa \quad \text{where} \quad Q = \sqrt{1+0.31\left(\frac{L}{\sqrt{2r_0 s_0}}\right)} \tag{11}$$

where: σ_u – ultimate tensile strength, d – depth of corroded region, L – longitudinal length of corroded region.

The failure begins in the thickness change area which causes stress concentration (Fig. 12) and propagates along the area of smaller thickness.

5.3. Pipeline without defect and with repair sleeve

In the third case, the undamaged pipe wrapped with glass fibre with epoxy resin is analysed. The thickness of composite wrap is 2.5 mm. The reinforcement causes a significant increase of burst pressure. In numerical simulations the maximum pressure until failure reaches 38.5 MPa and experimental test gives 39.65 MPa. The difference is about 3%. The failure starts by progressive composite fibres breakage in the area of cut out and leads to parallel to pipe axis fracture of the steel pipe. The character of structure failure is successively represented in numerical simulation.(see Fig. 13) (see Fig. 14)

5.4. Pipeline with defect and repair sleeve

The last test is performed on the defective-pipe repaired using epoxy filler and glass fibre reinforce composite wrap which consists 16 layers. The thickness of wrap is around 6.2 mm. In numerical calculation is represented by 8 elements trough thickness connected by cohesive interface. As a result of the repair process, the pipe sustained maximum pressure 29.4 MPa (Fig. 15). In the experimental test, the maximum burst pressure which pipe can resist is similar–29.06 MPa.

The increasing internal pressure causes composite fibre breakage at the external edge of the composite wrap and the following fracture of the steel pipe parallel to the pipe axis (Fig. 16).

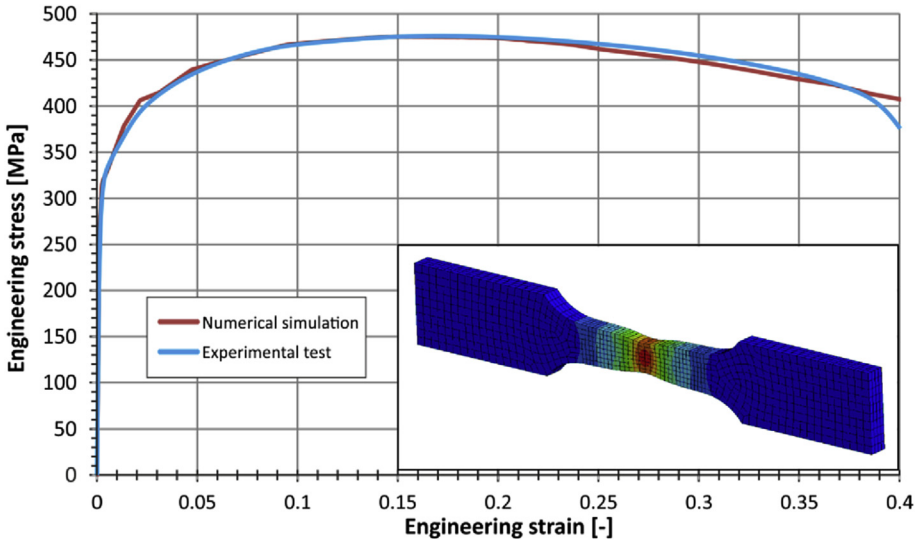

Fig. 8. Comparative curve of engineering strain and stress obtained during the experiment and numerical analysis.

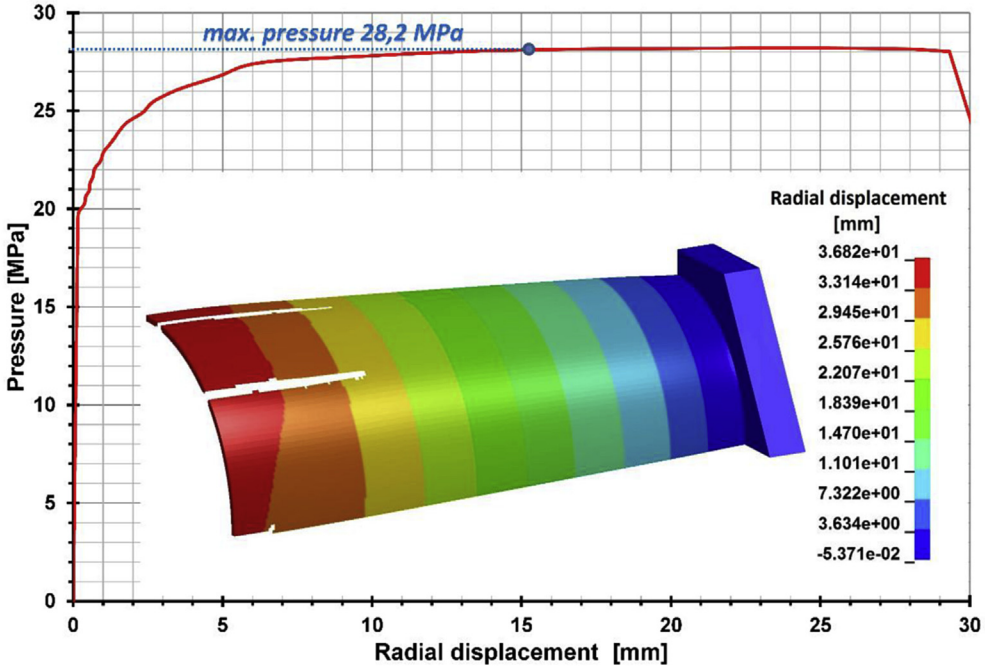

Fig. 9. Pressure versus maximum radial displacement – case 1.

6. Conclusions

The paper shows numerical and experimental burst pressure evaluation of the high pressure gas seamless hot-rolled steel pipe. In the study, several cases are considered: pipe without defect (Case 1), pipe with part-wall defect (Case 2), pipe without defect and with repair sleeve (Case 3), pipe with part-wall defect and repair sleeve (Case 4). The authors used a nonlinear explicit FE code with constitutive models which allows for steel and composite structure failure. The pressure loading based on airbag algorithm was also applied. The comparison of obtained results from all tests are presented in Fig. 17.

It can be observed that numerical analyses are in good agreement with experimental tests, however, the obtained values of maximum pressure until failure are slightly higher than from the real tests, especially in case 2. The differences between the results are probably caused by non-uniform thickness (imperfect manufacturing process) of the steel pipe in the experiment, quality of material, especially after the machining process and also simplifications in the numerical model such as discrete model symmetry, constant thickness and isotropic material behaviour. It also should be pointed out that the character of pipe fractures from numerical tests is very similar to cracks which occur in real pipes. Taking into account complexity of the simulated problems (steel and composite structure damage with delamination), authors decided that developed numerical models were accurate enough and adequate for the study of composite sleeve repair effectiveness.

The conducted analyses showed that local reduction of pipe wall

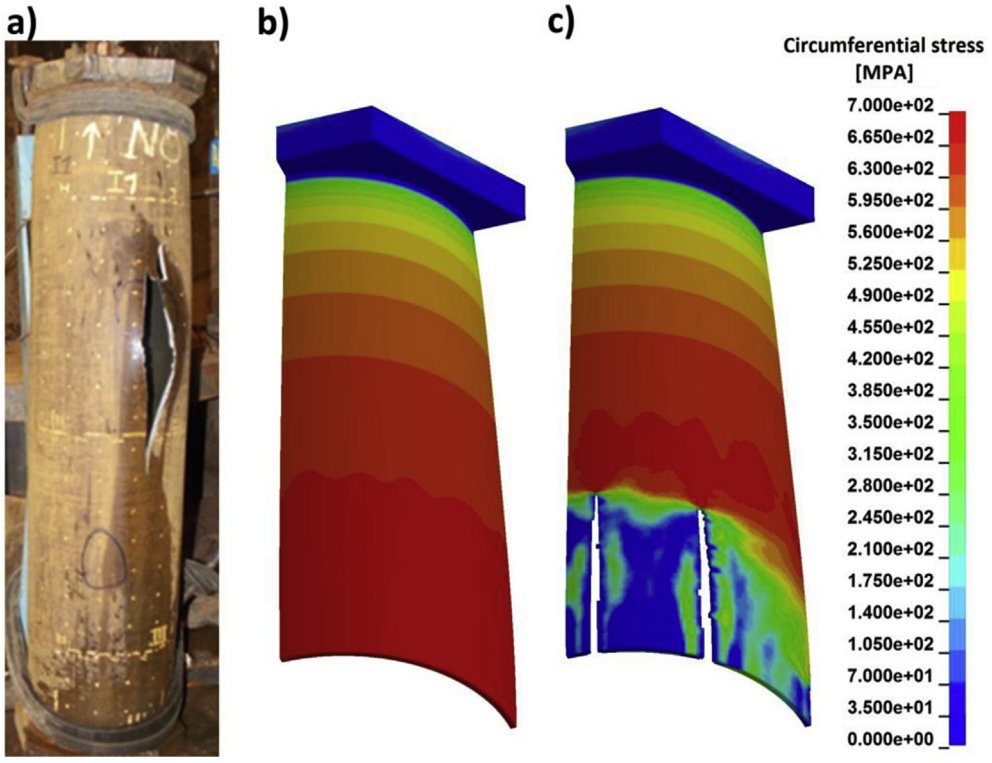

Fig. 10. Pipe after experimental test (a) and circumferential stresses from numerical analysis before (b) and after failure (c) – case 1.

Table 6
Comparison of results obtained by different methods.

	Experiment [MPa]	Numerical analysis [MPa]	Analytical calculations [MPa]	Numerical-experimental difference [%]	Numerical-analytical difference [%]
Maximum pressure until failure	27.59	28.2	28.413	2.1	0.74

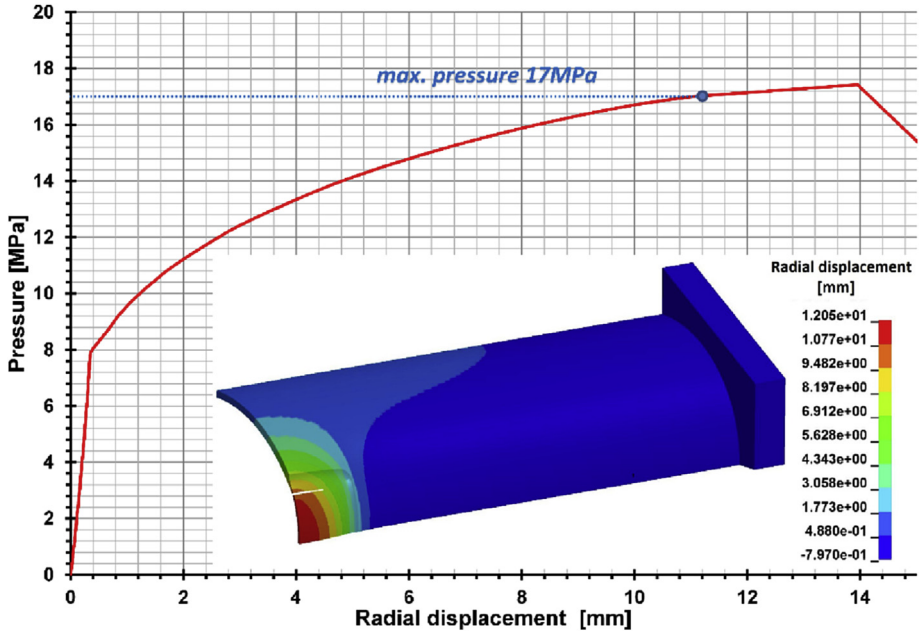

Fig. 11. Pressure versus maximum radial displacement – case 2.

Table 7
Comparison of results obtained by different methods.

	Experiment [MPa]	Numerical analysis [MPa]	Analytical calculations [MPa]	Numerical-experimental difference [%]	Numerical-analytical difference [%]
Maximum pressure until failure	13.8	17.0	15.26	18.8	10.2

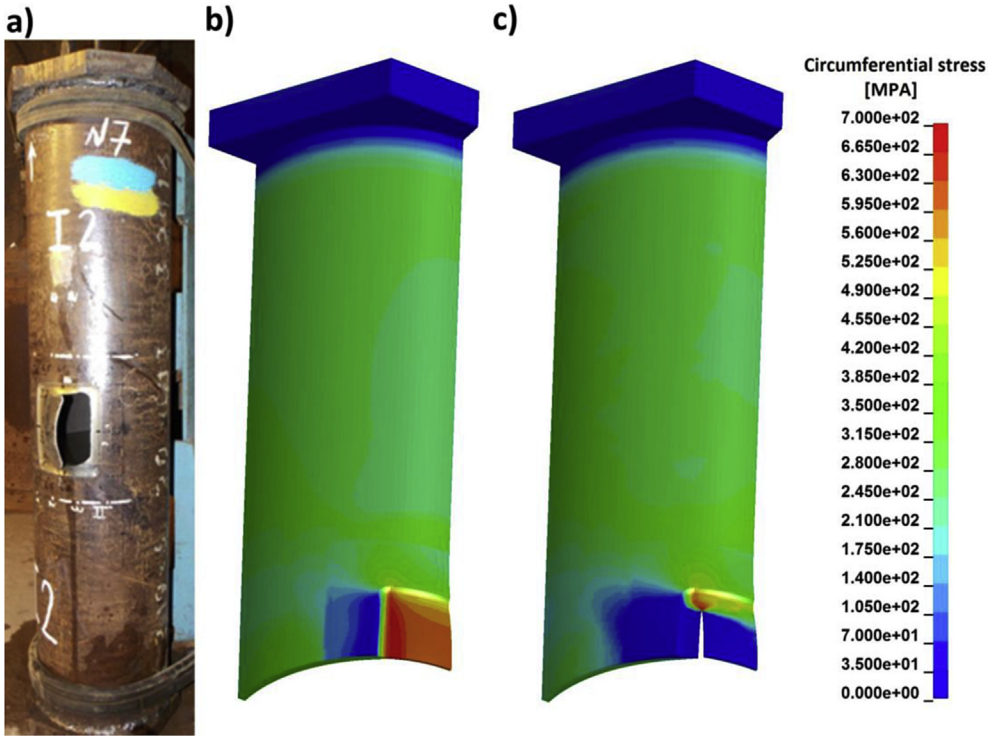

Fig. 12. Pipe after experimental test (a) and circumferential stresses from numerical analysis before (b) and after failure (c) – case 2.

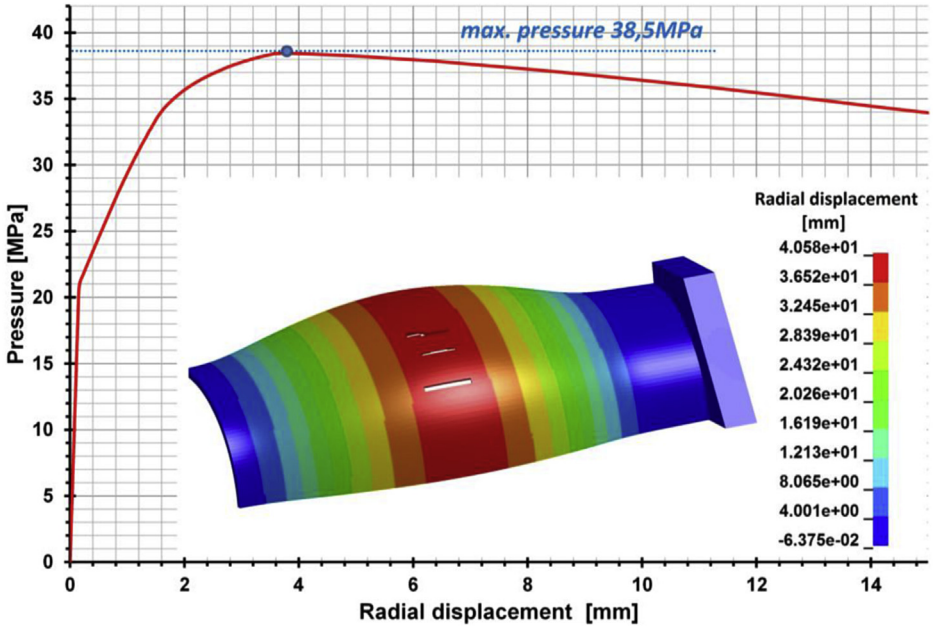

Fig. 13. Pressure versus maximum radial displacement – case 3.

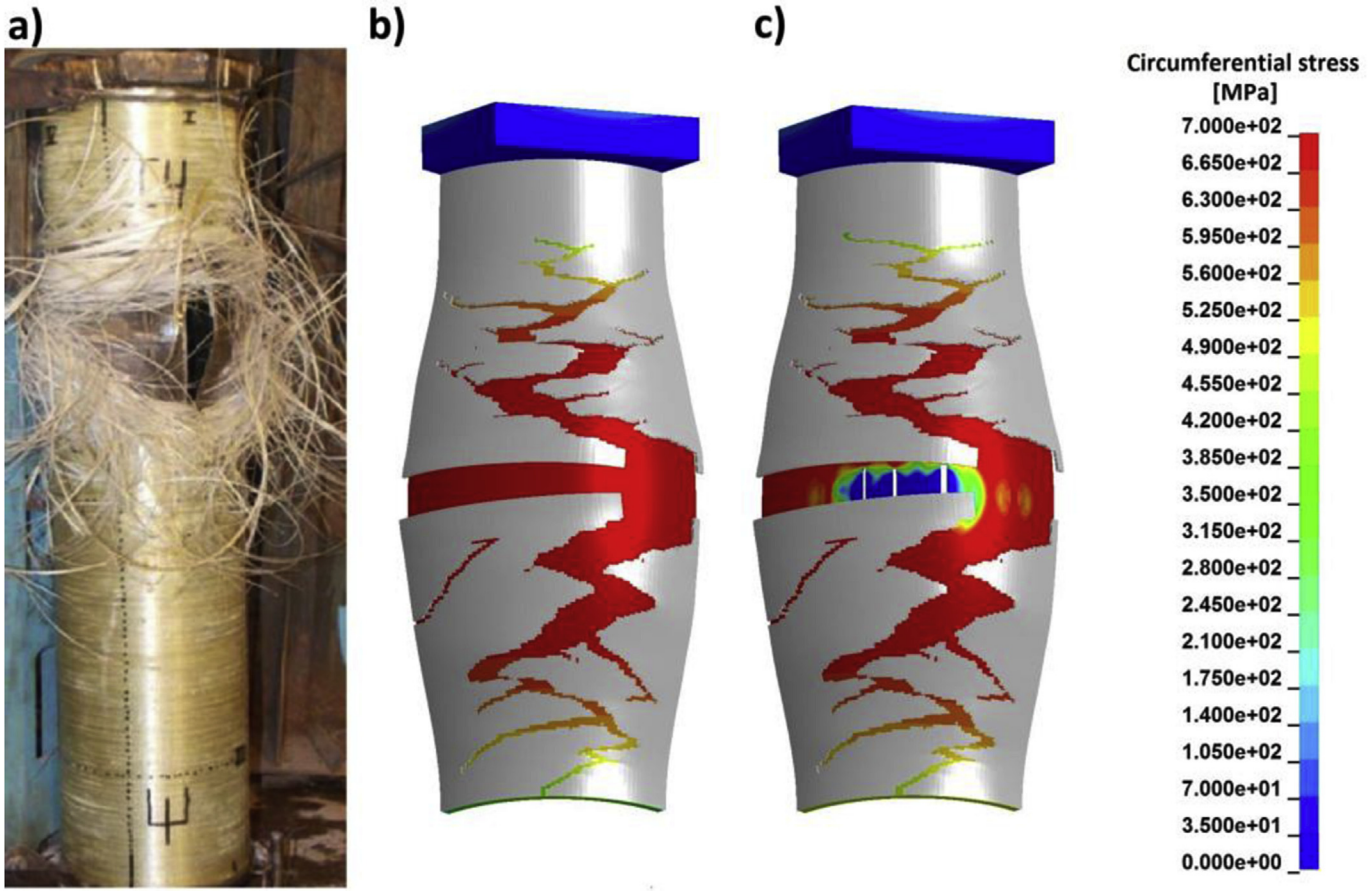

Fig. 14. Pipe after experimental test (a) and circumferential stresses from numerical analysis before (b) and after failure (c) – case 3.

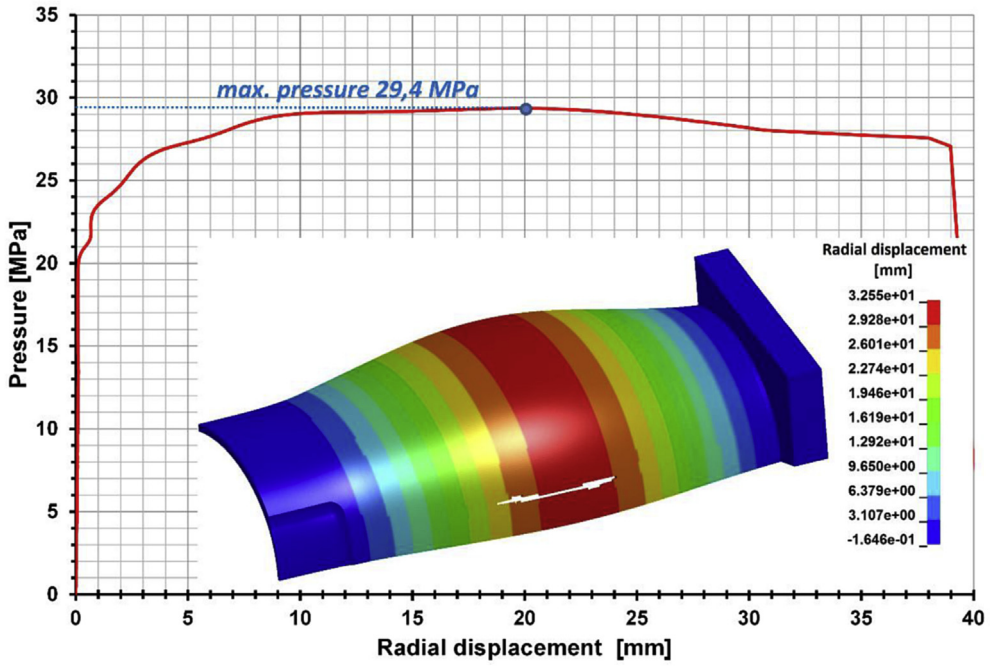

Fig. 15. Pressure versus maximum radial displacement – case 4.

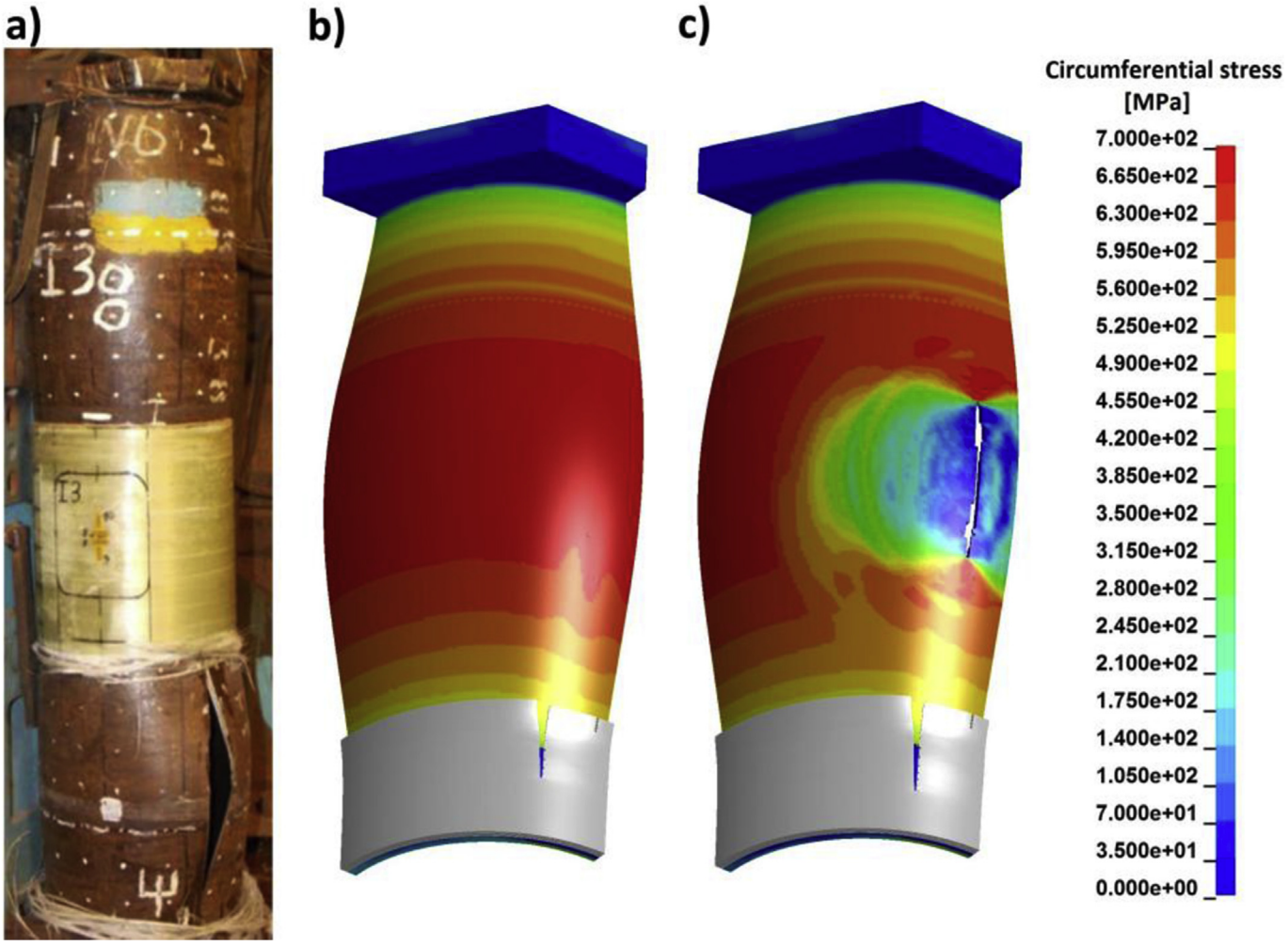

Fig. 16. Pipe after experimental test (a) and circumferential stresses from numerical analysis before (b) and after failure (c) – case 4.

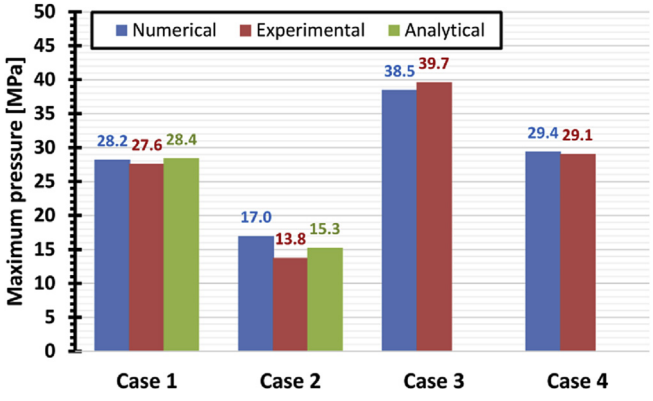

Fig. 17. Comparison of results from numerical and experimental studies.

thickness from 6 mm to 2.4 mm due to corrosion defect can reduce high pressure resistance by about 40%. At pressure over 17 MPa, the failure caused by stress concentration occurs in the thickness change area and results in local damage of the pipeline. Application of the repair system can eliminate this loss of resistance. The results of the burst pressure tests confirmed that, from the perspective of mechanical strength, the pipe with part-wall metal loss defect repaired by a fiber glass sleeve with cohesive epoxy resin with 6 mm thickness is more resistant than an original steel pipe considering burst pressure.

The developed models will be used in future analysis of repaired pipelines in different loading conditions.

Acknowledgements

The authors gratefully acknowledge the funding from Seventh Frame- work Program, Marie Curie Actions: “Innovative nondestructive testing and advanced composite repair of pipelines with volumetric surface defects”; Acronym: INNOPIPES; Proposal Number: 318874; Grant Agreement Number: PIRSES-GA-2012-318874.

References

[1] Witek M. An Assessment of the effect of steel pipeline wall losses on the maximum allowable operating pressure of a gas pipeline. J Pipeline Eng 2014;13:37–47.
[2] Witek M, Szałęga M. EMAT technology applied to high pressure gas pipelines diagnostic, SIGMA NOT Publishing House (in polish). Gaz Woda i Tech Sanit 2015;11:387–92.
[3] Cronin DS, Pick RJ. Prediction of the failure pressure for complex corrosion defects. Int J Press Vessels Pip 2002;79:279–87.
[4] Teixeira AP, Guedes Soares C, Netto TA, Estefen SF. Reliability of pipelines with corrosion defects. Int J Press Vessels Pip 2008;85:228–37.
[5] Moustabchir H, Azari Z, Hariri S, Dmytrakh I. Experimental and numerical study of stress-strain state of pressurised cylindrical shells with external defects. Eng Fail Anal 2010;17:506–14.

[6] Li X, Bai Y, Su C, Li M. Effect of interaction between corrosion defects on failure pressure of thin wall steel pipeline. Int J Press Vessels Pip 2016;138:8–18.
[7] Khalajestani MK, Bahaari MR. Investigation of pressurized elbows containing interacting corrosion defects. Int J Press Vessels Pip 2014;123–124:77–85.
[8] Xu LY, Cheng YF. Reliability and failure pressure prediction of various grades of pipeline steel in the presence of corrosion defects and pre-strain. Int J Press Vessels Pip 2012;89:75–84.
[9] Neacsa A, Dinita A, Baranowski P, Sybilski K, Ramadan Naim I, Małachowski J, et al. Experimental and numerical testing of gas pipeline subjected to excavator elements interference. J Press Vessel Technol 2016;138(3).
[10] Sahraoui Y, Khelif R, Chateauneuf A. Maintenance planning under imperfect inspection of corroded pipelines. Int J Press Vessels Pip 2013;104:76–82.
[11] Da Costa-Mattos HS, Reis JML, Sampaio RF, Perrut VA. An alternative methodology to repair localized corrosion damage in metallic pipelines with epoxy resins. Mater Des 2009;30:3581–91.
[12] Chapetti MD, Otegui JL, Manfredi C, Martins CF. Full scale experimental analysis of stress states in sleeve repairs of gas pipelines. Int J Press Vessels Pip 2001;78:379–87.
[13] Otegui JL, Cisilino A, Rivas AE, Chapetti M, Soula G. Influence of multiple sleeve repairs on the structural integrity of gas pipelines. Int J Press Vessels Pip 2002;79:759–65.
[14] Aleksander C, Ochoa OO. Extending onshore pipeline repair to offshore steel risers with carbon–fiber reinforced composites. Compos Struct 2010;92:499–507.
[15] Da Costa Mattos HS, Reis JML, Paim LM, da Silva ML, Lopes Junior R, Perrut VA. Failure analysis of corroded pipelines reinforced with composite repair systems. Eng Fail Anal 2016;59:223–36.
[16] GOST 8731-74 Seamless hot-deformed steel tubes – Technical requirements, Federal Agency on Technical Regulating and Metrology (2004).
[17] PN-EN ISO 3183. (E) Petroleum and natural gas industries – Steel pipe for pipe – line transportation systems, Polish Committee for Standardization. 2013. Warsaw 2013.
[18] Witek M. Possibilities of using X80, X100, X120 high-strength steels for onshore gas transmission pipelines. J Nat Gas Sci Eng 2015;27(1):374–84.
[19] American Water Works Association, Steel Pipe: A Guide for Design and Installation, fourth ed..
[20] Małachowski J, Hutsaylyuk V, Yukhumets P, Dmitryenko R, Beliaiev G, Prudkii I. Investigation of the stress-strain state of seamless pipe in the initial state. Archive Mech Eng 2014;61(4):595–607.
[21] Androno IN, Kuzbogev AS, Aginey RV. Resource of ground pipelines – I: factors that constraining resource. Stand Test Methods, Ukhta 2008:75–96.
[22] Malinin NN. Applied theory of plasticity and creep. second ed. 1975. Mechanical engineering, Moskow.
[23] Yukhymets P, Dmytriienko R. Protocols of Static Internal Pressure Test of Specimens I1 and I2 made of Pipe 219×6 (Steel 20), Innovative Non-destructive Testing and Advanced Composite Repair of Pipelines with Volumetric Surfaces Defects – INNOPIPES, Report WP 4 Task 4.2. The E.O. Paton Electric Welding Institute of The National Academy of Sciences of Ukraine; 2015.
[24] Hallquist JO, Dyna LS. Theory Manual. Livermore, USA: Livermore Publishing House; 2007.
[25] Chang FK, Chang KY. A progressive damage model for laminated composites containing stress concentrations. J Compos Mater 1987;21:834–55.
[26] Lakshmi R, Ravinder R. Investigation of interlaminar shear strength in carbon epoxy and carbon epoxy carbon nanotubes using experimental and finite element technique. Int J Eng Res Appl 2012;2:001–10.
[27] Guo Y. Eight-node solid element for thick shell simulations. Livermore Software Technology Corporation. Detroit: 6th International LS-Dyna conference; 2000.
[28] ASTM A370-14. Standard Test Methods and Definitions for Mechanical Testing of Steel Products. West Conshohocken, PA: ASTM International; 2014.
[29] Recommended Practice DNV-RP-F101 Corroded Pipelines, Det Norske Veritas, January 2015.